3D PIC simulations of current-driven instabilities in cylindrical magnetized jets

José Ortuño-Macías (jortuno@camk.edu.pl) & **Krzysztof Nalewajko** (knalew@camk.edu.pl)
Nicolaus Copernicus Astronomical Center, Polish Academy of Sciences, Bartycka 18, 00-716 Warsaw, Poland

CAMK PAN

Motivation

High-energy astrophysical phenomena commonly present regions with magnetic energy density that locally dominate the rest-mass density of matter. Such relativistic magnetizations can be converted to relativistic particle acceleration which is observed in the form of luminous non-thermal emission with photon energies extending into the gamma-ray band. Relativistically magnetized regions are expected in relativistic jets which may involve ordered magnetic fields with poloidal and toroidal components prone to kink and pinch instabilities [5]. Recently, first 3D kinetic simulations of cylindrical magnetized columns reported particle acceleration from two different magnetic field configurations, toroidal field supported by magnetic poloidal field [3] or by gas pressure [2]. In this work we introduce a radial profile of toroidal magnetic field that can be supported by a combination of poloidal magnetic field and gas pressure and investigate the particle acceleration mechanisms.

Simulation Setup

We used a modified version of the publicly available Particle-In-Cell code `Zeltron` [1]. We fit axisymmetric equilibria of outer radii $R_{out} = L_x/2$, centered along the axis $x = y = L_x/2$ where L_x is the physical size in x-axis of the computational domain. The equilibrium is based on the radial profile of toroidal magnetic field $B_\phi(r)$ in the form of a power-law with inner and outer cutoffs (see Figure 1):

$$B_\phi(r) = B_0 \left(\frac{r}{R_0}\right)^{\alpha_{B\phi}} C(s_{B\phi},\, r) C(s_{B\phi}, R_{out} - r) \tag{1}$$

where $C(s_{B\phi},\ r) = \frac{(r/R_0)^{s_{B\phi}}}{1+(r/R_0)^{s_{B\phi}}}$ with parameters $\alpha_{B\phi} \le 0$, $s_{B\phi} = 1 - \alpha_{B\phi}$, the *core radius* $R_0 = R_{out}/10 = L_x/20$. The initial equilibrium is provided by the electric current $j_z(r) = (c/4\pi r)\mathrm{d}(rB_\phi)/\mathrm{d}r$, as well as by the combination of poloidal magnetic field $B_z(r)$ and gas pressure $P(r)$. We introduce a constant parameter $f_{\rm mix} \in [0 : 1]$, which is the fraction of toroidal magnetic pressure supported by the gas pressure gradient (with the remainder supported by the poloidal magnetic pressure):

$$\frac{\mathrm{d}P}{\mathrm{d}r} = -f_{\rm mix}\frac{B_\phi}{4\pi r}\frac{\mathrm{d}(rB_\phi)}{\mathrm{d}r} \tag{2}$$

$$\frac{\mathrm{d}B_z^2}{\mathrm{d}r} = -(1 - f_{\rm mix})\frac{2B_\phi}{r}\frac{\mathrm{d}(rB_\phi)}{\mathrm{d}r} \tag{3}$$

with the initial density profile $n(r) = P(r)/\Theta_0 m_e c^2$, where $\Theta_0 = kT_0/m_e c^2$. Additionaly we investigated different density ratio, $n_{\rm ratio} \equiv n_{\rm max}/n_{\rm min}$, which is an indicator of the magnetization ($\sigma = B_0^2/4\pi\Theta_0 n m_e c^2$); higher density ratio provides higher magnetization.

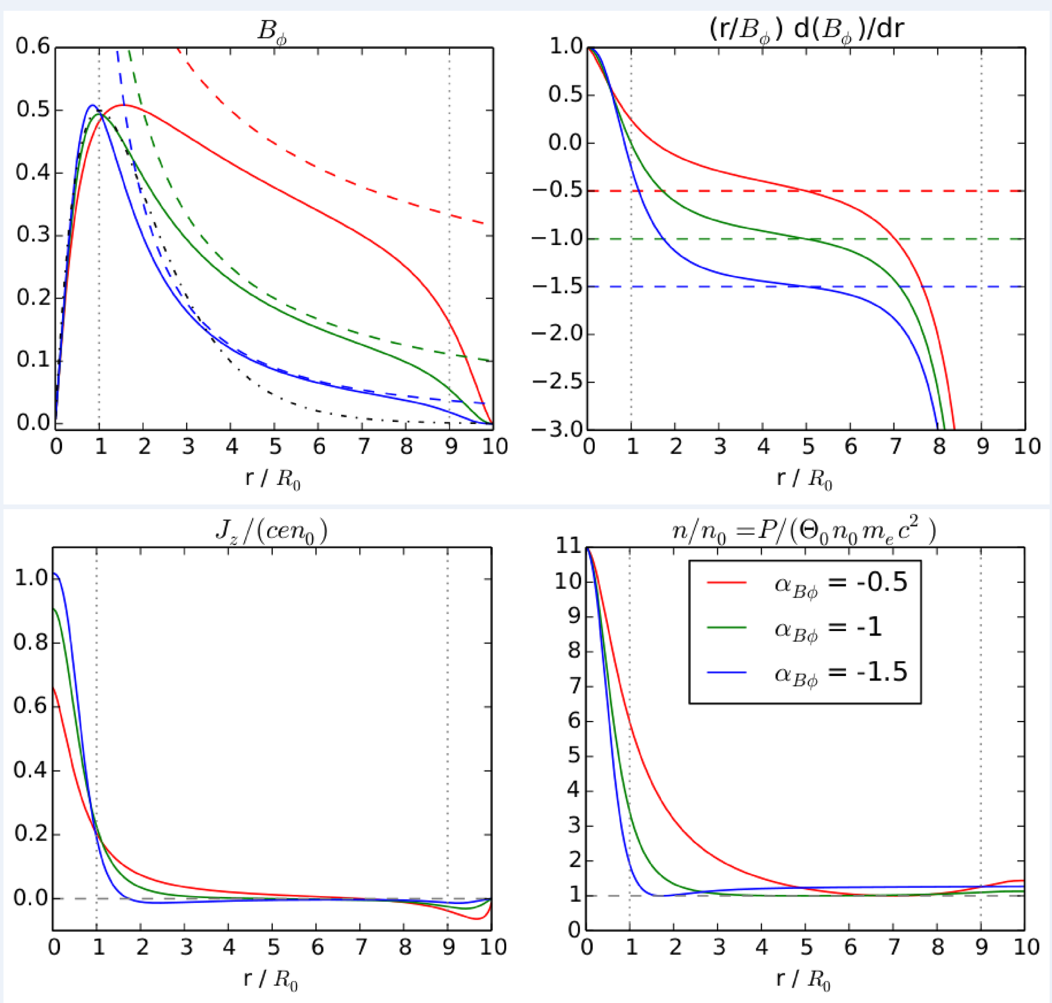

Figure 1: *Top left*: radial profiles of toroidal field $B_\phi(r)$ compared for $\alpha_{B\phi} = -0.5, -1, -1.5$. Power-law profiles without cutoffs are shown with dashed lines. *Top right*: "local $\alpha_{B\phi}$"- logarithmic derivative of $B_\phi(r)$. *Bottom left*: poloidal current density. *Bottom right*: gas density profile (for $f_{\rm mix} = 1$ case).

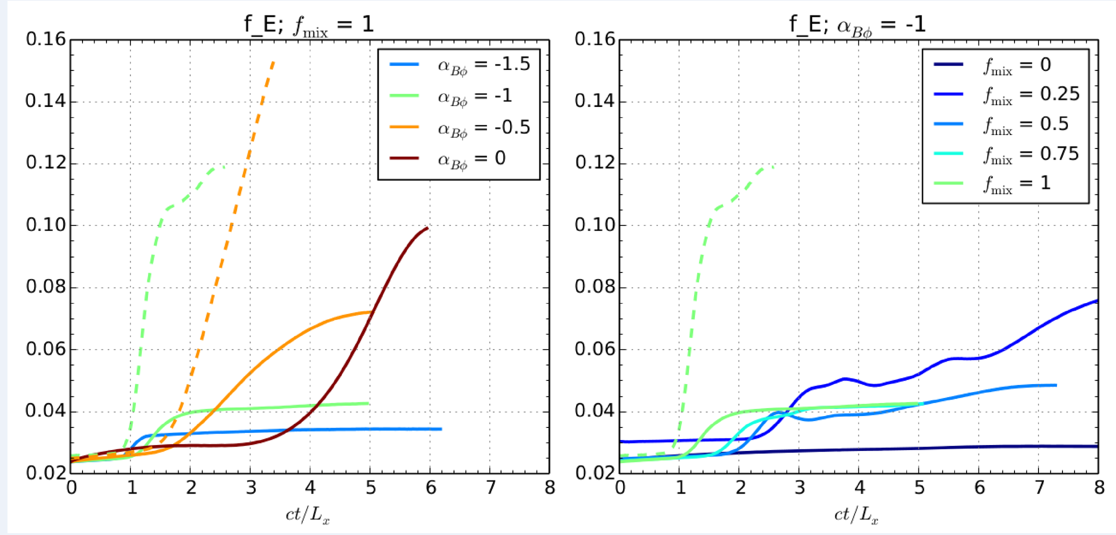

Figure 2: Non-thermal energy fraction evolution with time. We present two panels corresponding to two series of simulations were the power law index, $\alpha_{B\phi}$ (*left panel*) and the fraction of toroidal magnetic pressure supported, $f_{\rm mix}$ (*right panel*) are explored. In solid lines we show simulations with $n_{\rm ratio} = 10$ (which reach peak magnetizations of $\sigma \sim 0.5$) and in dashed lines $n_{\rm ratio} = 100$ simulations (with peak magnetization values $\sigma \sim 5$).

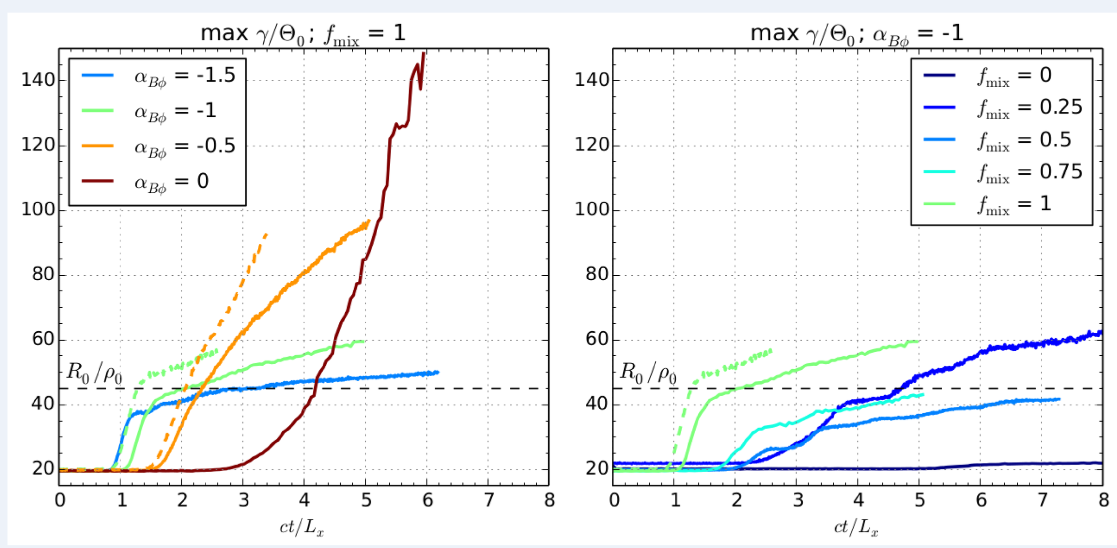

Figure 3: Time evolution of the maximum particle energy for the two series of simulations. The horizontal black dashed line shows the confinement energy (see Alves et al. 2018). Linestyles are as in Fig. 2.

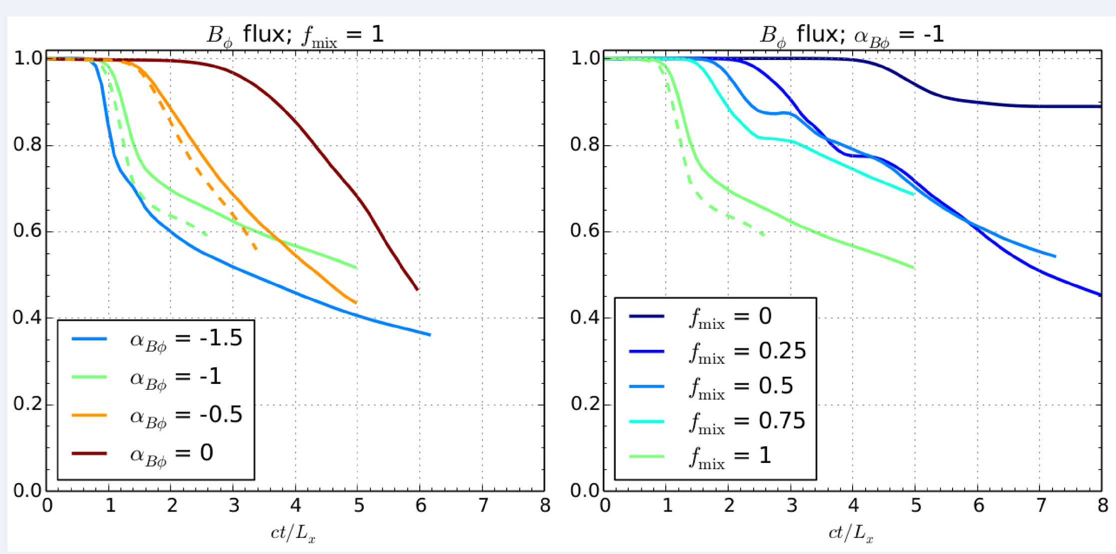

Figure 4: Time evolution of the toroidal magnetic flux dissipation. Linestyles are as in Fig. 2.

Acknowledgements

We thank Dmitri A. Uzdensky, Mitchell C. Begelman, Alex Chen and Gregory Werner for insightfull comments. Simulations were performed at the supercomputer `Prometheus` located at the Academic Computer Centre 'Cyfronet' of the AGH University of Science and Technology in Krakow, Poland (PLGrid grants `pic19, plgpic20, ehtsim`). This work is supported by the Polish National Science Centre Grant 2015/18/E/ST9/00580.

Results

- Kink mode (m=1) is the dominant instability mode for the configurations where there is some poloidal magnetic field support, $f_{\rm mix} < 1$; kink and pinch (m=0) mode have similar amplitudes for gas pressure supported cases, $f_{\rm mix} = 1$.
- Particle acceleration results from ideal MHD electric fields ($\mathbf{E} \perp \mathbf{B}$), dominated by E_z component, which is partially countered by deceleration by E_ϕ for the configurations with initial B_z, i.e., $f_{\rm mix} < 1$.
- Maximum particle energies are limited to the confinement energy, however for shallow toroidal magnetic profiles, $\alpha_{B\phi} \ge -1$ they exceed it
- For magnetic profiles with $\alpha_{B\phi} \le -1$, magnetic dissipation proceeds in two phases, a rapid phase due to the ideal **E** and a slow phase due to turbulence.

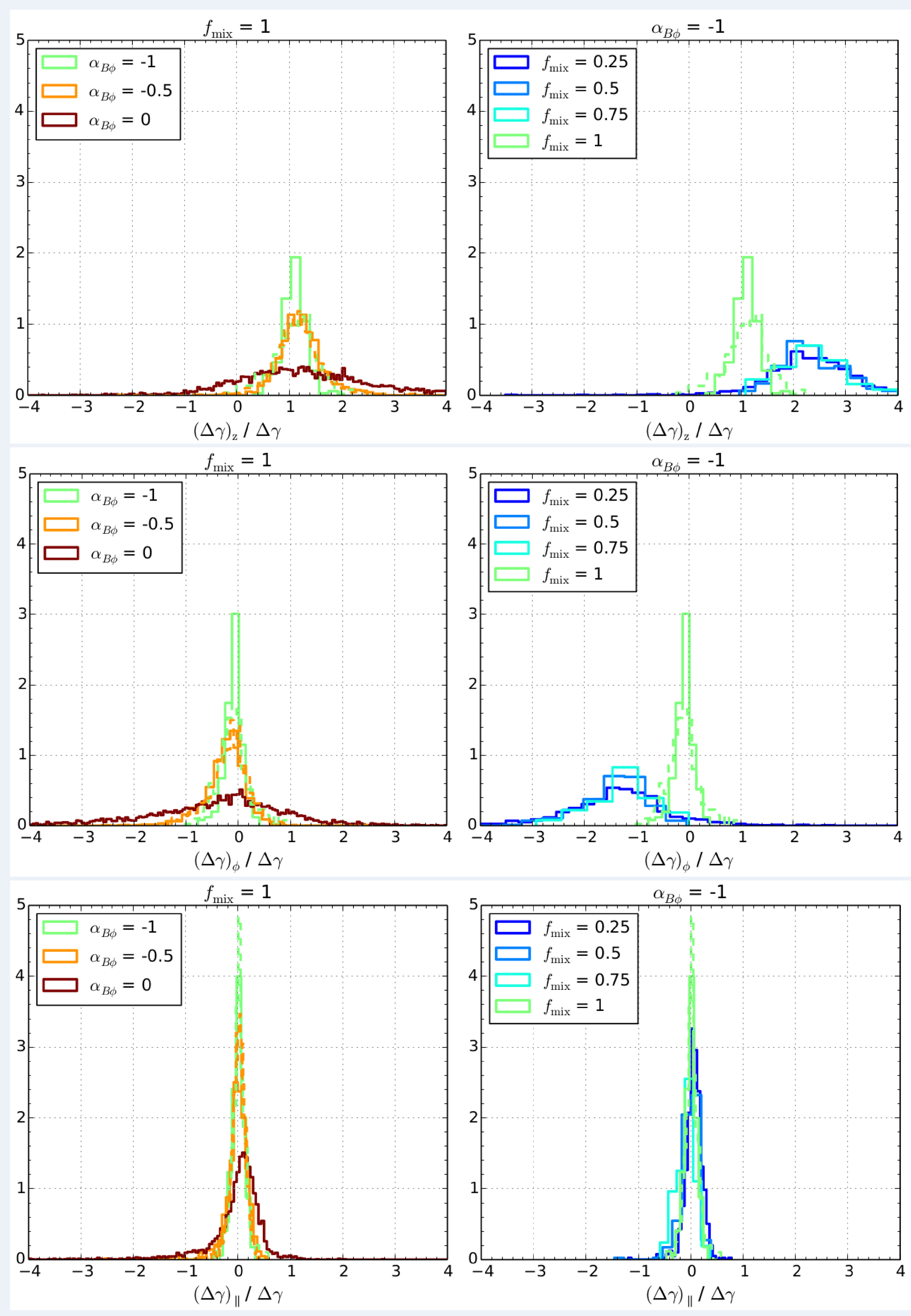

Figure 5: Distribution of energy gain due to the z, ϕ and $\parallel$ (parallel to **B** field) components of the electric field, **E**. All the energy gain components are normalized to the total work resulting from **E**.

References

[1] Cerutti, B., Werner, G. R., Uzdensky, D. A. & Begelman, M. C. 2013, ApJ, 770, 147

[2] Alves, E.P., Zrake, J., & Fiuza, F. 2018, Phys. Rev. Lett., 121, 245101

[3] Davelaar, J., Philippov, A. A., Bromberg, O., Singh, C. B. 2020, ApJ, 896, L31

[4] Bromberg, O., Singh, C. B., Davelaar, J., Philippov, A. A. 2019, ApJ, 884, 39

[5] Begelman, M. C. 1998, ApJ, 493, 291